

Quantum effects in a cylindrical carbon-nanotube capacitor

This article has been downloaded from IOPscience. Please scroll down to see the full text article.

2007 J. Phys.: Condens. Matter 19 365218

(<http://iopscience.iop.org/0953-8984/19/36/365218>)

View [the table of contents for this issue](#), or go to the [journal homepage](#) for more

Download details:

IP Address: 129.252.86.83

The article was downloaded on 29/05/2010 at 04:37

Please note that [terms and conditions apply](#).

Quantum effects in a cylindrical carbon-nanotube capacitor

Kazuyuki Uchida, Susumu Okada, Kenji Shiraishi and Atsushi Oshiyama

Center for Computational Sciences and Institute of Physics, University of Tsukuba,
1-1-1 Tennodai, Tsukuba 305-8577, Japan
and
CREST, Japan Science and Technology (JST) Agency, 4-1-8 Honcho, Kawaguchi,
Saitama 332-0012, Japan

E-mail: kuchida@comas.frsc.tsukuba.ac.jp

Received 1 December 2006, in final form 19 January 2007

Published 24 August 2007

Online at stacks.iop.org/JPhysCM/19/365218

Abstract

We have theoretically investigated the electric polarization and capacitance in a nano-scale coaxial-cylindrical capacitor made of a double-walled carbon nanotube, (6, 0)@(36, 0), using a first-principles density-functional method with the enforced Fermi-energy difference scheme. We show that the distribution of the accumulated charge in the inner tube is quantum-mechanically spilled outward, while that in the outer tube is penetrating inward. Reflecting these charge spills, the electrostatic capacitance of the system is larger than what would be expected from classical theory. Furthermore, the total capacitance of the system is smaller than the electrostatic capacitance, which is another quantum effect showing large contributions from the DOS of the electrodes to the capacitance. We believe that these two quantum effects in the capacitance are important for the successful design of carbon-nanotube devices.

1. Introduction

Carbon nanotubes (CNTs) have attracted a great deal of attention as a most promising material for the fabrication of future nanoelectronics devices. Many theoretical studies of the conductance in CNTs have already been performed with the aim of achieving successful designs for CNT devices [1]. However, theoretical investigations of the *capacitance* in CNT-based systems have only just begun [2, 3], despite the manifestly important role played by gate *capacitors* in field-effect transistors (FETs), which are the most significant element of electronic-device technologies.

In this work we discuss the electric polarization and capacitance of a double-walled CNT, (6, 0)@(36, 0), as a nano-scale coaxial-cylindrical capacitor. For electron-state calculations we

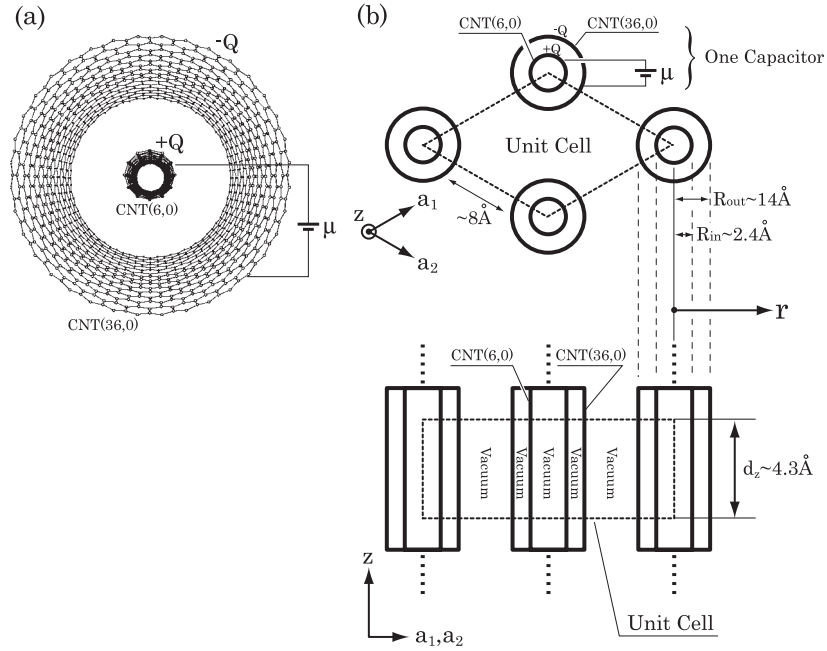


Figure 1. (a) The atomic structure and (b) a schematic picture of the calculated model, (6, 0)@(36, 0). These tubes have infinite lengths. Their tube-wall radii are R_{in} ($\sim 2.4 \text{ \AA}$) and R_{out} ($\sim 14 \text{ \AA}$). We use the three-dimensional periodic boundary condition. The length of the unit cell along the tube axis is $d_z \sim 4.3 \text{ \AA}$. Each tube is seamless in this direction. In the directions perpendicular to the tube axis, on the other hand, neighbouring capacitors are separated by a vacuum by more than $\sim 8 \text{ \AA}$, which ensures that the present system simulates an isolated coaxial-cylindrical capacitor of CNTs.

use a first-principles density-functional method [4] with the enforced Fermi-energy difference scheme [5, 6]. This is one of the first steps towards the successful design of gate capacitors in CNT-based FETs. We can also regard the coaxial-cylindrical geometry of the present system as an ultimately scaled down model of the gate capacitor in a surrounding-gate transistor (SGT) [7], that is, a representative example of three-dimensional FETs which have been developed to pursue higher integration degree of electronic circuits.

In the following we show that the distribution of the accumulated charge in the inner tube is quantum-mechanically spilled outward, while that in the outer tube is penetrating inward. Reflecting these quantum spills, the electrostatic capacitance of the system is larger than would be expected from classical theory. Furthermore, the total capacitance of the system is smaller than the electrostatic capacitance, which is another quantum effect showing a large contribution to the capacitance from the DOS of the electrodes. We believe that these two quantum effects in the capacitance are important for the successful design of CNT devices.

2. Model

We show (a) the atomic structure and (b) the schematic picture of the calculated model in figure 1. The inner tube is a (6, 0) CNT, and the outer one is a (36, 0) CNT. They have infinite lengths, and serve as the electrodes of the nano-scale coaxial-cylindrical capacitor in this work. The radii of these tubes are $R_{in} \sim 2.4 \text{ \AA}$ and $R_{out} \sim 14 \text{ \AA}$, respectively. We apply a

finite bias μ (Fermi-energy difference) between them so that holes ($+Q$) and electrons ($-Q$), respectively, are injected into them. The total charge neutrality of the system is maintained throughout this work ($+Q - Q = 0$), despite this electron transfer from one electrode to the other. These electrodes are separated from each other by a cylindrical vacuum region between them, where the tails of the one-electron wavefunctions of the occupied electron states are sufficiently damped.

As is also illustrated in figure 1(b), we use the three-dimensional periodic boundary condition in this work. The unit cell contains 168(= 144 + 24) carbon atoms. One axis of the unit cell is parallel to the tubes, whereas the other two axes of the cell are perpendicular to them. The length of the unit cell along the tube axis is $d_z \sim 4.3$ Å. Each tube is seamless in this direction. On the other hand, in the directions perpendicular to the tube axis, neighbouring capacitors are separated by a vacuum. The capacitor–capacitor distance is large enough (more than ~ 8 Å) in these directions to avoid wavefunction overlap among them. Also, the electrostatic interactions between the accumulated charges ($\pm Q$) are confined between the two electrodes within each capacitor. Our system therefore simulates an isolated coaxial-cylindrical capacitor of CNTs.

3. Method

For theoretical analyses of the electric polarization and the capacitance of the CNT capacitor, we performed first-principles electron-state calculations based on the density-functional theory (DFT) [4] and the local-density approximation (LDA). To describe the many-body effects of interacting electrons, we use the exchange–correlation energy density parametrized by Perdew and Zunger [8]. We also use the Vanderbilt ultra-soft pseudo-potential [9], which enables us to describe the 2s and 2p electron states reliably and at reasonable computing cost. By using the conjugate-gradient (CG) structural optimization method, we optimized the atomic structure of the CNT capacitor with the constraint of coaxiality under the bias voltage $\mu = 0$. Structural relaxations after application of the bias are neglected in this work, which mimics the response of the present capacitor to high-frequency bias. The cut-off energy of the plane-wave basis set to expand the one-electron wavefunctions is chosen as 36 Ryd. The theoretical calculations are performed with the Tokyo *Ab initio* Program Package (TAPP), which has been developed by our group [11, 12].

To calculate charge-accumulated states of the capacitor, we used the enforced Fermi-energy difference formalism [5, 6]. In this methodology, we minimize the *free* energy $F_{\text{DFT}}[\rho(r)]$ defined by

$$F_{\text{DFT}}[\rho(r)] = E_{\text{DFT}}[\rho(r)] - \mu \cdot \Delta N[\rho(r)], \quad (1)$$

which considers the work $\mu \cdot \Delta N[\rho(r)]$ supplied by a power source¹. This is in contrast to the minimization of the energy $E_{\text{DFT}}[\rho(r)]$ usually performed in conventional first-principles electron-state calculations.

In the term of the supplied work, μ is the applied bias voltage (i.e. the Fermi-energy difference) between the two electrodes of the capacitor, and $\Delta N[\rho(r)]$ is the number of electrons transferred from one electrode to the other, calculated as

$$\Delta N[\rho(r)] = \int v(r) \cdot \Delta \rho(r) dr \quad (2)$$

¹ In the classical electrostatic limit, $Q = CV$ (charge-accumulated state) can be obtained by minimizing the free energy defined by $F(Q) = Q^2/2C - QV$. Here, $Q^2/2C$ is the energy of the capacitor with an electric polarization of $\pm Q$. QV is the work supplied by the power source.

in this work. Here, $\Delta\rho(r)$ is the distribution of the accumulated electrons defined by

$$\Delta\rho(r) = \rho(r) - \rho_0(r), \quad (3)$$

where $\rho_0(r)$ and $\rho(r)$ are the total electron density before and after application of the bias. Also, we define $v(r)$ by

$$v(r) = \begin{cases} 0, & \text{for } r \in \text{the one electrode,} \\ & \text{and} \\ 1, & \text{for } r \in \text{the other electrode,} \end{cases} \quad (4)$$

which describes the boundary plane dividing the system into two parts belonging to one electrode and the other electrode, respectively. This boundary plane can be arbitrarily chosen in the vacuum region between the two electrodes of the capacitor, as far as where the tails of the one-electron wavefunctions of the occupied electron states are sufficiently damped. In the present work, we have chosen this to be at the middle of the inner and outer-tube-wall radii.

The electron density is calculated by

$$\rho(r) = \sum_{\epsilon'_n \leq \epsilon'_{\text{pFermi}}} |\phi'_n(r)|^2, \quad (5)$$

with the pseudo-Fermi level $\epsilon'_{\text{pFermi}}$ chosen as $\epsilon'_{\text{pFermi}} = \epsilon_{\text{Fermi}}^{\text{one}} = \epsilon_{\text{Fermi}}^{\text{other}} - \mu$, so that the total charge neutrality of the system is maintained ($+Q - Q = 0$) despite the inter-electrode electron transfer after application of the bias. The Kohn–Sham equation [10] is also modified as follows:

$$[\hat{H}_{\text{KS}} + w(r)]\phi'_n(r) = \epsilon'_n \phi'_n(r), \quad (6)$$

where

$$w(r) = -\mu \cdot v(r) = \begin{cases} 0, & \text{for } r \in \text{the one electrode,} \\ & \text{and} \\ -\mu, & \text{for } r \in \text{the other electrode,} \end{cases} \quad (7)$$

effectively describes the biased chemical potentials of the electrons applied to the system. Note that atomic nuclei do not feel this $w(r)$, though they have positive charges. In this meaning, the effective potential $w(r)$ is quite different from the usual electric field externally applied to the system. In the terminology of the present paper we do not include $w(r)$ in the local potential. We also exclude the contribution from $w(r)$ when physically interpreting the calculated spectra $\{\epsilon'_n\}$. When using the ultra-soft pseudo-potentials, we have to also restore the deficit in the norm of pseudo wavefunctions according to the conventional treatments [9].

4. Results and discussions

First, we show the distribution of the accumulated charge $\Delta\rho_\mu(r)[= \rho_\mu(r) - \rho_0(r)]$ calculated under the bias voltage $\mu = +245$ meV. The projection of $\Delta\rho_\mu(r)$ onto the radial coordinate is plotted in figure 2(a). Here, the quantity of the accumulated charge is $\pm Q = \pm e \times \Delta N[\rho_\mu(r)] = \pm 0.0242e$ per unit cell. As can be seen from this figure, the distribution of accumulated charge in the inner tube is quantum-mechanically spilled outward from the inner-tube-wall radius R_{in} , while that in the outer tube is penetrating inward from the outer-tube-wall radius R_{out} . These tendencies are consistent with previous discussions in other CNTs [3].

The profile of the distribution $\Delta\rho_\mu(r)$ strongly suggests that carbon $2p_z$ orbitals (i.e. frontier orbitals of CNTs) are closely concerned with this charge accumulation. The spill lengths of the accumulated charge in the inner and outer tubes ($\Delta \sim 1$ Å) are, however, about

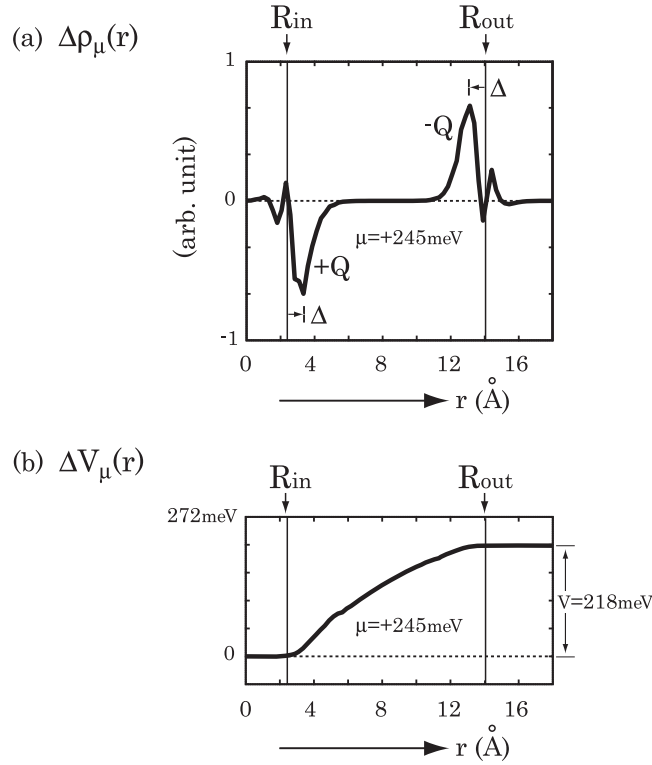


Figure 2. (a) Distribution of the accumulated charge $\Delta\rho_\mu(r)$, defined by $\Delta\rho_\mu(r) = \rho_\mu(r) - \rho_0(r)$. Δ ($\sim 1 \text{ \AA}$) is a measure of the spill length of the accumulated charge. (b) Variation in the local potential $\Delta V_\mu(r)$, defined by $\Delta V_\mu(r) = V_\mu(r) - V_0(r)$.

twice as large as that of the carbon $2p_z$ orbitals. Thus, to understand the distribution of the accumulated charge, we have to consider the bias-induced deformation of the wavefunctions. In other words, dielectric polarizations of the occupied electron states are also important for understanding the length of the quantum spill. In general, plane-wave basis sets are suitable for accurately describing such a deformation of the wavefunctions if compared with LCAO (linear combination of atomic orbitals) basis sets.

Next we discuss the bias-induced variation in the local potential, defined by

$$\Delta V_\mu(r) = V_\mu(r) - V_0(r). \quad (8)$$

In figure 2(b), we show the angular mean of $\Delta V_\mu(r)$ calculated under the bias voltage $\mu = +245 \text{ meV}$. Most of the $\Delta V_\mu(r)$ originates from the variation in the Hartree potential. Thus, we can regard V , defined by

$$V = \Delta V_\mu(R_{out}) - \Delta V_\mu(R_{in}), \quad (9)$$

as the electrostatic potential shift induced by the charge accumulation.

We can observe that the V value (218 meV) is smaller than the μ value (245 meV). This discrepancy between the applied bias voltage μ (inter-electrode Fermi-energy difference) and the resultant electrostatic potential shift V is explained by the Fermi-level shifts originated from the Fermi statistics; when a finite-value DOS is occupied by newly injected electrons (holes), the Fermi-energy levels shifts upward (downward) within the DOS of each CNT electrode [13]. The total bias μ is explained by the summation of the Fermi-level shift within the DOS of

the inner electrode, that within the outer electrode, and the relative energy shift of the DOS structures of the electrodes brought about by the electrostatic potential shift V . In macro-scale systems V is dominant in μ . However, in nano-scale systems, contributions from the μ - V discrepancy can be large and play an important role when estimating the capacitance value. We have indeed estimated the values of the capacitance C and its electrostatic component C_0 per unit cell, defined by

$$C = dQ/d\mu, \quad \text{and} \quad C_0 = dQ/dV, \quad (10)$$

respectively. By using the data at $\mu = 245$ meV, they are

$$C \sim 1.6 \times 10^{-20} \text{ F}, \quad (11)$$

and

$$C_0 \sim 1.8 \times 10^{-20} \text{ F}. \quad (12)$$

As is straightforwardly understood from the aforementioned discussions on the applied bias μ and the resultant potential shift V , the reason why C is smaller than C_0 (μ is larger than V) is due to the contributions from the DOS of the electrodes. This is essentially a quantum effect, and can never be explained just from the classical electrostatics. The small width of the vacuum region separating the two electrodes of the capacitor, and the relatively small DOS values around the Fermi levels, make the C - C_0 discrepancy conspicuous [13]. Detailed analysis, including an in-depth comparison with the DOS structures of the electrodes and discussions on the bias dependence of the capacitance, will be given elsewhere [14]. Note that the capacitance obtained in experiments corresponds to C , *not* to C_0 . This is because the bias μ , supplied by the power source, is the input parameter of experiments.

We also point out that the electrostatic capacitance C_0 is larger than the classical expectation C_{classic} , calculated as

$$C_{\text{classic}} = \frac{2\pi\epsilon_0 d_z}{\ln(R_{\text{out}}/R_{\text{in}})} \sim 1.4 \times 10^{-20} \text{ F}. \quad (13)$$

Here ϵ_0 is the dielectric constant of a vacuum. We can attribute this deviation to the quantum-mechanical spill of the accumulated charge; actually, we can reproduce the C_0 value as

$$\frac{2\pi\epsilon_0 d_z}{\ln[(R_{\text{out}} - \Delta)/(R_{\text{in}} + \Delta)]} \sim 1.8 \times 10^{-20} \text{ F}, \quad (14)$$

by considering the spill length of the accumulated charge Δ (~ 1 Å). In other words, we can say that the effective radius of the inner tube, $R_{\text{in}}^{\text{eff}}$ ($= R_{\text{in}} + \Delta$), is larger than it appears, while that of the outer tube, $R_{\text{out}}^{\text{eff}}$ ($= R_{\text{out}} - \Delta$), is smaller than it seems, because of the quantum-mechanical spill of the accumulated charges.

5. Conclusion

In conclusion, we have theoretically investigated the electric polarization and the capacitance of a double-walled carbon nanotube capacitor, (6, 0)@(36, 0), by using a first-principles density-functional method with the enforced Fermi-energy difference scheme. We have shown that the distribution of the accumulated charge in the inner tube is quantum-mechanically spilled outward, while that in the outer tube penetrates inward. Reflecting these spills, the electrostatic capacitance of the system is larger than expected from classical electrostatics. Furthermore, the total capacitance of the system is smaller than the electrostatic capacitance, which is another quantum effect showing the large contribution from the DOS of the electrodes to the capacitance. We believe that these two quantum effects in the capacitance are important for the successful design of CNT devices.

Acknowledgments

We thank T Endoh, K Natori, Y Fujimoto, J-I Iwata and K Kamiya for their stimulating discussions throughout this work. This work is partly supported by CREST-JST, and grant-in-aid from MEXT under contract number 17064002. Computations were done at the Academic Computing and Communications Center, University of Tsukuba, Institute for Solid State Physics, University of Tokyo, and at the Research Center for Computational Science, Okazaki National Institute.

References

- [1] Ando T 2005 *J. Phys. Soc. Japan* **74** 777
- [2] Pomorski P, Roland C, Guo H and Wang J 2003 *Phys. Rev. B* **67** 161404(R)
- [3] Meunier V, Kaninin S V, Shin J, Baddorf A P and Harrison R J 2004 *Phys. Rev. Lett.* **93** 246801
- [4] Hohenberg P and Kohn W 1964 *Phys. Rev.* **136** B864
- [5] Uchida K, Kageshima H and Inokawa H 2005 *e-J. Surf. Sci. Nanotech.* **3** 453 see <http://www.sssj.org/ejsnt/>
- [6] Uchida K, Kageshima H and Inokawa H 2006 *Phys. Rev. B* **74** 035408
- [7] Masuoka M, Endoh T and Sakuraba H 2002 *Presented at 4th IEEE Int. Caracas Conf. on Devices, Circuits and Systems (Aruba, April 2002)* pp C015-1–5
- [8] Perdew J P and Zunger A 1981 *Phys. Rev. B* **23** 5048
- [9] Vanderbilt D 1990 *Phys. Rev. B* **41** 7892
- [10] Kohn W and Sham L J 1965 *Phys. Rev.* **140** A1133
- [11] Tsukada M *et al* 1983–2006 *Computer Program Package (TAPP)* University of Tokyo, Tokyo, Japan
- [12] Yamauchi J, Tsukada M, Watanabe S and Sugino O 1996 *Phys. Rev. B* **54** 5586
- [13] Büttiker M 1993 *J. Phys.: Condens. Matter* **5** 9361
- [14] Uchida K, Okada S, Shiraishi K and Oshiyama A to be published